Microchimica Acta
https://doi.org/10.1007/s00604-017-2663-8

ORIGINAL PAPER

Ultrathin $NiCo_2O_4$ nanowalls supported on a 3D nanoporous gold coated needle for non-enzymatic amperometric sensing of glucose

Weiwei Li[1] · Hui Qi[2] · Baogang Wang[3] · Qiyu Wang[4] · Shuting Wei[1] · Xiaolin Zhang[1] · Ying Wang[1] · Lei Zhang[1] · Xiaoqiang Cui[1]

Received: 15 December 2017 / Accepted: 31 December 2017

Abstract

A disposable needle-type of hybrid electrode was prepared from a core of stainless steel needle whose surface was modified with a 3D nanoporous gold/$NiCo_2O_4$ nanowall hybrid structure for electrochemical non-enzymatic glucose detection. This hybrid electrode, best operated at 0.45 V (vs. SCE) in solutions of pH 13 has a linear response in the 0.01 to 21 mM glucose concentration range, a response time of <1 s, and a 1 μM detection limit (at an S/N ratio of 3). The remarkable enhancement compared to the solid gold/$NiCo_2O_4$ and stainless steel/$NiCo_2O_4$ hybrid electrodes in electrochemical performance is assumed to originate from the good electrical conductivity and large surface area of the hybrid electrode, which enhance the transport of mass and charge during electrochemical reactions. This biosensor was also applied to real sample analysis with little interferences. The electrode is disposable and considered to be a promising tool for non-enzymatic sensing of glucose in a variety of practical situations.

Keywords Stainless steel · Gold needle electrode · $NiCo_2O_4$ nanosheets · Electrodeposition · Electrochemical glucose biosensor · Blood serum · Glucose electrooxidation · Electrocatalyst · Biosensor · Electrochemical alloying/dealloying

Introduction

As one of the most prevalent worldwide diseases, diabetes elicits a demand for low-cost and high-performance electrochemical glucose biosensors [1]. Numerous research efforts have been attempted to developing non-enzymatic glucose biosensors since the conventional enzymatic glucose biosensors are suffering from drawbacks of high cost, instability, and complicated immobilization techniques [2, 3]. Nanostructured noble metals [4–6], transition metallic oxides [7–10], sulphides [11–13], and phosphides [14–16] have been extensively developed for the applications of non-enzymatic biosensor. Among them, noble metallic nanostructrues is expensive and easy to be poisoned by chloride ions and intermediates during glucose oxidation process [17], while sulphides and phosphides are normally toxic. The mixed transition metal oxide of $NiCo_2O_4$ is one promising material for non-enzymatic biosensors due to its high biocompatibility and excellent electrochemical catalytic activity [18, 19]. The performance of these nanostructured transition oxides were usually hindered by their low intrinsic electronic conductivity and the problem of aggregation [20].

Constructing 2D nanowalls on the conductive substrates were effective to improve the intrinsic electronic conductibility and prevent the aggregation [21–23]. The traditional conductive substrates of ITO, Ni foam, and carbon fiber paper are unsuitable for integrating implantable or wearable devices. Nanoporous gold (NPG), a three-dimensional (3D) nanostructured metal, has shown advantages in biosensors as a conductive substrate due to its high conductivity and large surface area [24, 25]. However, the pure gold NPG wires are soft and expensive for disposable high-throughput glucose detection.

Electronic supplementary material The online version of this article (https://doi.org/10.1007/s00604-017-2663-8) contains supplementary material, which is available to authorized users.

✉ Xiaoqiang Cui
xqcui@jlu.edu.cn

[1] State Key Laboratory of Automotive Simulation and Control, Department of Materials Science, Jilin University, Changchun 130012, China

[2] The Second Hospital of Jilin University, Changchun 130041, People's Republic of China

[3] The First Hospital of Jilin University, Changchun 130041, People's Republic of China

[4] Key Laboratory for Renewable Energy, Institute of Physics, Chinese Academy of Sciences, Beijing 100190, China

Published online: 24 January 2018

We describe here a disposable needle-type stainless steel coated with a solid gold layer for NPG needle that is supported with ultrathin $NiCo_2O_4$ nanowalls for non-enzymatic electrochemical glucose sensing. The structure and the fabrication process of the NPG/$NiCo_2O_4$ hybrid electrode are illustrated in Scheme 1. A thin solid gold layer and the stainless steel needle was used to lower down the cost and improve the mechanical strength compared to the pure gold wire, respectively. The gold surface layer was etched into the NPG layer by an electrochemical etching process, and the $NiCo_2O_4$ nanowalls were subsequently grown onto the nanoporous channel of NPG. This NPG/$NiCo_2O_4$ hybrid electrode exhibited a linear range of 0.01 to 21 mM and a fast response time of less than 1 s for the detection of glucose. The enhanced sensing performance was ascribed to the combination of the 3D interconnected nanoporous channel structure of NPG and the ultrathin nanowalls of $NiCo_2O_4$, which provided a large electrochemical active surface area (ECSA) and enhanced the transport of glucose and electrons.

Experimental section

Materials

The reagents used in the experiment were of analytical grade and were used without further purification. *D*-(+)-glucose was obtained from Sigma-Aldrich (St Louis, USA, http://www.sigma-aldrich.com). Acetone and ethanol were purchased from Beijing Chemical Reagent (Beijing, China, http://www.pvc123.com/b-beijinghuagong/). All other reagents, including nickel nitrate hexahydrate ($Ni(NO_3)_2{\cdot}6H_2O$), cobalt nitrate hexahydrate ($Co(NO_3)_2{\cdot}6H_2O$), benzyl alcohol (BA), zinc chloride ($ZnCl_2$), sodium hydroxide (NaOH), sodium chloride (NaCl), fructose, mannose, maltose, sucrose, lactose, uric acid (UA), *L*-ascorbic acid (AA), dopamine hydrochloride (DA), urea, and acetamidophenol (AP), were purchased from Sinopharm Chemical Reagent (Shanghai, China, http://www.sinoreagent.com). The stainless steel (SS) needles and the solid gold (Au) coated needles were gifted from San Meditech Co., Ltd., China. Deionized water were used from a Milli-Q system (18.2 MΩ·cm at 25 °C) throughout the experiments.

Preparation of the NPG needles

NPG needles were prepared by an in-situ electrochemical alloying/dealloying method according to a published procedure with appropriate modifications [20, 26]. In a typical synthesis, a multi-sweep cyclic voltammetry (CV) electrochemical alloying/dealloying process was performed with a three-electrode electrochemical setup in the potential range from 1.88 V to −0.72 V at a scan rate of 10 $mV{\cdot}s^{-1}$ at 120 °C in 100 mL BA electrolyte containing 1.5 M $ZnCl_2$. A Zn plate, a Zn wire, and five solid gold needles was used as the auxiliary electrode, the reference electrode, and the working electrode, respectively. After the optimized 40 cycles CV scanning, the NPG needles were taken out and cleaned for 10 min with acetone, ethanol, and deionized water in sequence. NPG needles were then transferred into an HNO_3 solution (HNO_3: H_2O = 1:4, *v*/v) and sonicated for 5 min, and soaked for three days to remove the residual Zn. Finally, the treated NPG needles were sonicated in deionized water and dried for 1 h in vacuum oven at 60 °C.

NPG/$NiCo_2O_4$ hybrid needle electrodes

The synthesis of the ultrathin $NiCo_2O_4$ nanowalls on the nanoporous gold needles was performed via a two-step method. Typically, in the first step, the Ni-Co bimetallic hydroxide precursor was electrodeposited by a chronoamperometric technique on an optimized NPG needle as the working electrode, a platinum plate as the counter electrode, and a saturated calomel electrode (SCE) as the reference electrode in a glass cell. The deposition electrolyte consisted of 5 mM $Ni(NO_3)_2{\cdot}6H_2O$ and 10 mM $Co(NO_3)_2{\cdot}6H_2O$ dissolved in 25 mL of deionized water. The deposition potential of −0.8 V was held constant for 420 s, and the green-colored NPG needle was carefully rinsed several times with deionized water, finally dried in air at 60 °C for 2 h. In the second step, the sample was placed in a porcelain boat and calcined at 300 °C in air for 2 h with a ramp rate of 1 $°C{\cdot}min^{-1}$ to transform the deposited material into ultrathin $NiCo_2O_4$ nanosheets.

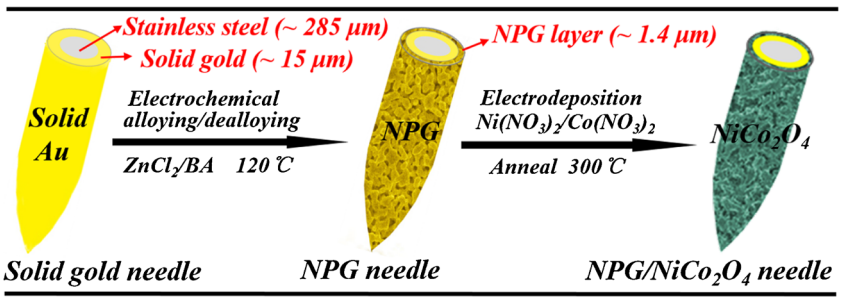

Scheme 1| Schematic illustration for the synthesis of NPG/$NiCo_2O_4$ needle-type electrode

Characterization

The scanning electron microscopy (SEM) images, elemental mapping images, and energy dispersive X-ray spectroscopy (EDX) were obtained using a field- emission scanning electron microscope (Hitachi, SU8010). Transmission electron microscopy (TEM), high-resolution transmission electron microscopy (HRTEM), and selected-area electron diffraction (SAED) measurements were performed using a JEM-2100F transmission electron microscope (JEOL Co., Japan). X-ray diffraction (XRD) patterns were collected with a Bragg-Brentano diffractometer (D8-tools, Germany) equipped with a Cu-Kα source emitting at 0.15418 nm. X-ray photoelectron spectroscopy (XPS) measurements were performed with a monochromatic Al-Kα (14, 866 eV) radiation source and a hemisphere detector with an energy resolution of 0.1 eV, and the spectra were acquired with an ESCALAB-250 instrument (Thermo Fisher Scientific, USA). The Raman spectra were captured with a micro-Raman spectrometer (Renishaw) using a 514 nm wavelength laser.

Electrochemical testing

The electrochemical measurements were performed using a three-electrode setup on a CHI650D electrochemical workstation (Shanghai Chenhua, China, http://chi.instrument.com.cn). The $NiCo_2O_4$-modified needle electrode fixed on a metal plate was used as the working electrode, while the saturated calomel electrode and platinum plate were used as the reference electrode and counter electrode, respectively. The electrolyte was a 0.1 M NaOH aqueous solution saturated with nitrogen. The CV curves were measured in the 20 mL electrolyte with and without 5 mM glucose. The amperometric responses of electrodes were recorded by successive addition of glucose under steady-state conditions at a potential of 0.45 V vs. SCE.

Results and discussion

Characterization of the NPG needle

The NPG needles were prepared by a multi-sweep CV electrochemical alloying/dealloying process. The number of etching cycles shows great influence on the formation of NPG as shown in Fig. S1. An increasing number of cycles reduces the characteristic width of the NPG ligaments. Obviously, the etched of solid gold was incomplete with less etch cycles, while an excess of etching cycles would decompose the surface of NPG and lead to the too small of NPG ligaments width, even formed the fractured NPG. The ECSA test indicates that the 40 cycles NPG needles show the largest surface active area, which is of approximately 20 times than the solid gold needles (Fig. S2). This optimized NPG needles with 40 cycles CV scanning have a rough surface with a moderate 3-D continuous nanoporous channel structure with the ligaments width of approximately 200 nm (Fig. S1c). The trace amount of zinc has little effects on the properties of NPG (Fig. S3, S4). The structure information of the prepared needle was investigated by SEM as shown in Fig. 1. A representative cross-sectional SEM image and the corresponding elemental mapping show that the core is 300-μm-diameter stainless steel that is coated with a 15 μm solid gold layer (Fig. 1a-d). The thickness of the NPG layer was determined to be of 1.4 μm by a statistical method (Fig. 1e). A photograph shows the exceptional mechanical flexibility of this NPG needle electrode (Fig. 1f). The structure of the prepared NPG needle is consistent with the design in Scheme 1.

Morphology and composition characterization of the NPG/$NiCo_2O_4$ hybrid electrode

$NiCo_2O_4$ nanowalls were synthesized by an electrodeposition and post-calcination process [19]. The whole electrochemical process as follows: the deposition potential was held at −0.8 V versus SCE to reduce NO_3^- ions adsorbed the electrode surface to generate hydroxide ions (Eq. 1). Then the Ni^{2+} and Co^{2+} ions reacted with locally generated hydroxide ions to form bimetallic hydroxide on the surface of electrodes according to Eq. 2. Finally, the formed hydroxides were oxidized to black spinel $NiCo_2O_4$ supported on the NPG (Eq. 3).

$$NO_3^- + 7H_2O + 8e^- \rightarrow NH_4^+ + 10OH^- \quad (1)$$

$$xNi^{2+} + 2xCo^{2+} + 6xOH^- \rightarrow Ni_xCo_{2x}(OH)_{6x} \quad (2)$$

$$Ni_xCo_{2x}(OH)_{6x} + 1/2xO_2 \rightarrow xNiCo_2O_4 + 3xH_2O \quad (3)$$

The morphology and electrochemical activity were investigated by SEM and CV technique, respectively. SEM results (Fig. 2a-d) show that the $NiCo_2O_4$ nanowalls are directly formed on the NPG ligaments within the continuous nanoporous channels and the loading amount of $NiCo_2O_4$ increases with increasing electrodeposition time. Only a small amount of $NiCo_2O_4$ nanowalls were grown on the NPG at 300 s (Fig. 2b). A large amount of $NiCo_2O_4$ nanosheets on the surface had blocked the nanoporous structure with 540 s growth (Fig. 2d). CV curves indicate the NPG/$NiCo_2O_4$ hybrid electrodes with 420 s exhibit the highest electrochemical activity (Fig. 2e), which is in good agreement with the SEM result of a moderate amount of $NiCo_2O_4$ with 420 s growth in Fig. 2c. This enhanced electrochemical activity of NPG/$NiCo_2O_4$ hybrid electrode is attributed to the nanoporous structure of NPG. TEM image of the NPG/$NiCo_2O_4$ interface indicates that the $NiCo_2O_4$ nanosheets have end-bonded contact with the Au ligaments (Fig. 2f), overcoming the poor electrical conductivity of $NiCo_2O_4$. The morphologies of the $NiCo_2O_4$

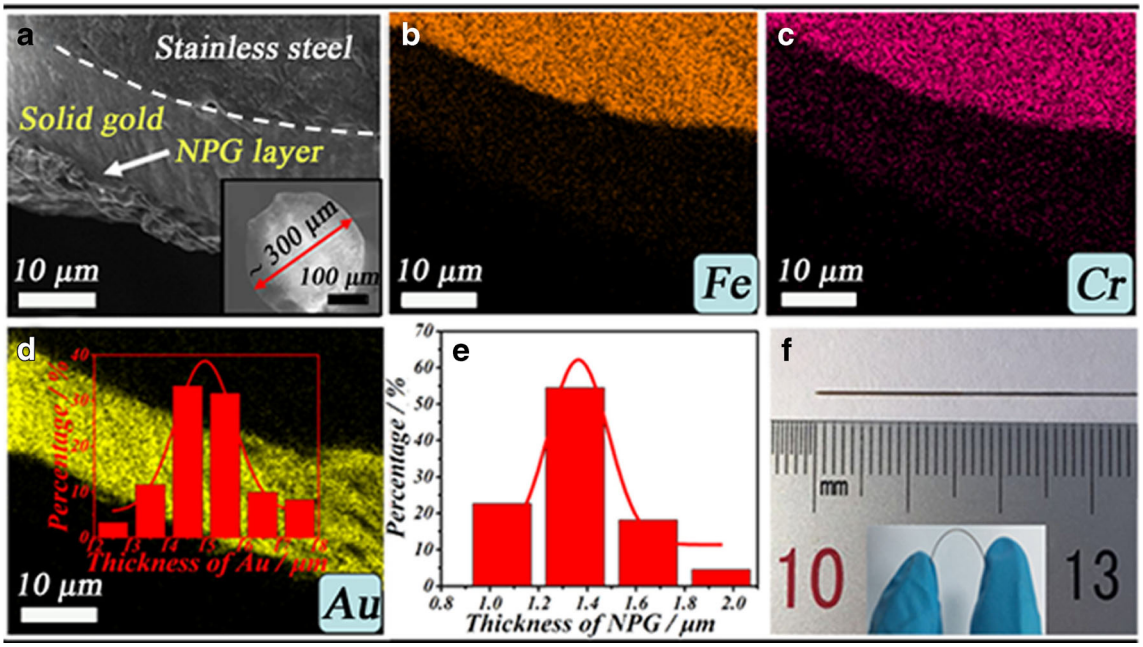

Fig. 1 Characterization of nanoporous gold needle. a Cross-sectional SEM image of an NPG needle. **b**, **c**, and **d** are the corresponding elemental mapping images of a). The inset in **d** and **e** are the corresponding thickness distribution diagram of the solid gold layer and the NPG layer, respectively. **f** Photograph of the NPG needle

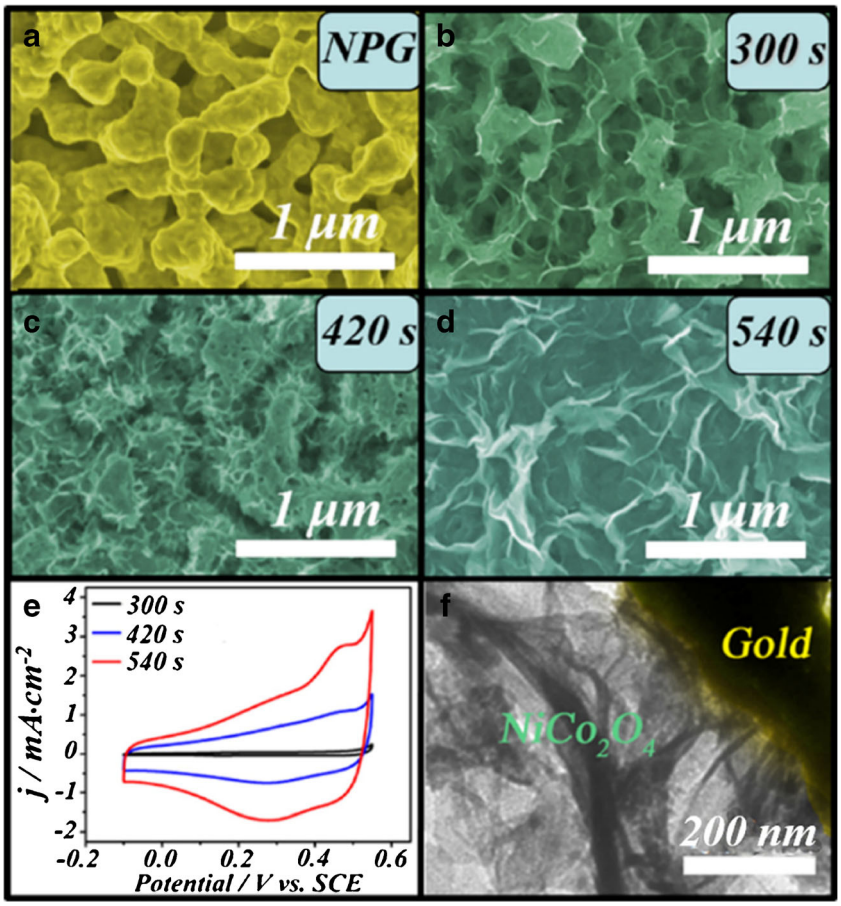

Fig. 2 Morphological characterization. Top-view SEM images of $NiCo_2O_4$/NPG electrodes at various deposition times: **a** bare NPG, **b** 300 s, **c** 420 s, and **d** 540 s. **e** CV curves of NPG/$NiCo_2O_4$ needles with varying deposition times at a scan rate of 50 $mV \cdot s^{-1}$. **f** TEM image of the $NiCo_2O_4$/NPG interfacial structure

in the TEM images also demonstrate the ultrathin nature of the nanosheets. The composition characterization by XRD, TEM XPS, and Raman spectra confirmed the successful synthesis of NPG/$NiCo_2O_4$ hybrid (Fig. S5–6).

Electrochemical characterization of the NPG/$NiCo_2O_4$ hybrid electrode

The electrochemical behavior of the hybrid electrodes was investigated by CV both in the absence (dotted line) and in the presence (solid line) of 5 mM glucose (Fig. 3a). It is apparent that the electrochemical response current of the NPG/$NiCo_2O_4$ hybrid electrode is much larger than that of the Au/$NiCo_2O_4$ (blue curves) and SS/$NiCo_2O_4$ (black curves) hybrid electrodes both in the absence and presence of glucose. The glucose oxidation current of NPG/$NiCo_2O_4$ is much larger than that of NPG (Fig. S7). The high performance of NPG/$NiCo_2O_4$ is attributed to the hierarchical nanoporous structure of the hybrid electrode (Fig. S8). The possible reaction processes were shown as follows: During the anodic scan, the $NiCo_2O_4$ on the electrode surface was converted to CoOOH, CoO_2, and NiOOH with a pair of broad redox peaks at about 0.45 V due to the oxidation reaction (Eqs. 4, 6, and 7), and the glucose molecules were rapidly oxidized to glucolactone by the NiOOH and CoO_2 species at about 0.45 V (Eqs. 5 and 8) [27–30].

$$NiCo_2O_4 + OH^- + H_2O \rightarrow NiOOH + 2CoOOH + e^- \quad (4)$$

$$2NiOOH + \text{glucose} \rightarrow 2NiO + \text{glucolactone} + H_2O \quad (5)$$

$$NiO + OH^- - e^- \rightarrow NiOOH \quad (6)$$

$$CoOOH + OH^- \rightarrow CoO_2 + H_2O + e^- \quad (7)$$

$$2CoO_2 + \text{glucose} \rightarrow 2CoOOH + \text{glucolactone} \quad (8)$$

A perfect linear relationship between the peak current density and the scan rate indicates that the process of electron transfer is indeed a surface-controlled electrochemical process as shown in Fig. 3b [28, 31]. The electron transfer resistance of the hybrid needles was investigated by EIS in Fig. 3c. The diameter of the semicircle of the NPG/$NiCo_2O_4$ (red curve) is visibly much smaller than that of the Au/$NiCo_2O_4$ (blue curve) and SS/$NiCo_2O_4$ (black curve), indicating that the electron transfer ability of the NPG/$NiCo_2O_4$ is significantly improved by incorporating NPG [13, 32]. The ECSA of the modified electrodes was also estimated by evaluating the electrochemical double-layer capacitance in Fig. 3d, which was derived from the CV measurements in Fig. S9 [33, 34]. The ECSA of the NPG/$NiCo_2O_4$ hybrid material was estimated to

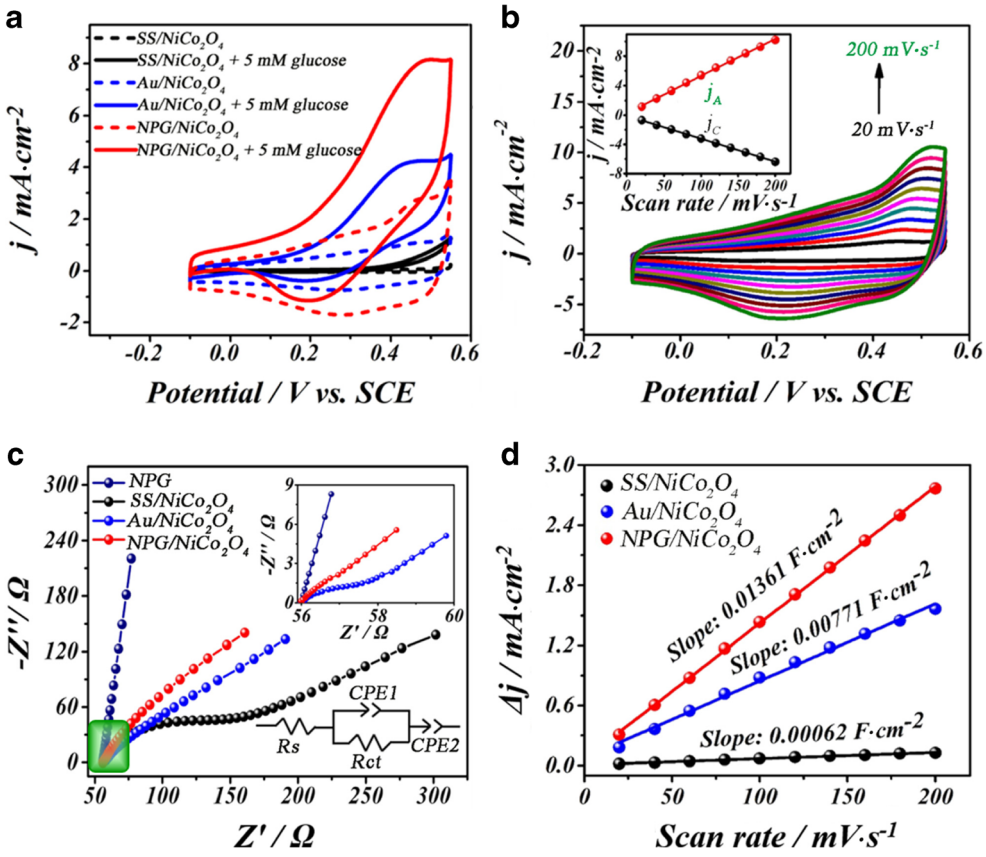

Fig. 3 Electrochemical characterization. a CV curves of the hybrid electrodes in the absence (dotted line) and the presence (solid line) of 5 mM glucose in a 0.1 M NaOH solution at scan rate 50 $mV \cdot s^{-1}$. **b** CV curves of the NPG/$NiCo_2O_4$ electrode at different scan rates. Inset: Plots of the peak current density as a function of scan rates. **c** Nyquist plots of the prepared products in a 0.1 M KCl solution containing 5 mM $[Fe(CN)_6]^{3-/4-}$ from 10^5 Hz to 1 Hz. Inset: the enlarged curves of NPG, Au/$NiCo_2O_4$, and NPG/$NiCo_2O_4$. **d** Capacitive J versus scan rates for the modified electrodes

be approximately 2 and 28 times than that of the Au/$NiCo_2O_4$ and SS/$NiCo_2O_4$, respectively, revealing that the NPG/$NiCo_2O_4$ hybrid nanostructure exposed more catalytic active sites, which improved the electrochemical performance. We attributed the superior activity of the NPG/$NiCo_2O_4$ to its advantageous nanostructure.

Electrochemical performance of the glucose biosensor

Amperometric detection of glucose

A typical comparison of amperometric responses for the SS/$NiCo_2O_4$, Au/$NiCo_2O_4$, and NPG/$NiCo_2O_4$ hybrid electrodes with successive addition of the glucose is shown in Fig. 4a. The results indicate that the NPG/$NiCo_2O_4$ hybrid electrode has a higher amperometric response than both SS/$NiCo_2O_4$ and Au/$NiCo_2O_4$ hybrid electrodes. The corresponding calibration curves are presented in Fig. 4b, error bars are the RSD of 3 times detection. The results show that the curves for both the SS/$NiCo_2O_4$ and Au/$NiCo_2O_4$ hybrid electrodes fit a hyperbolic function over the whole concentration range. The NPG/$NiCo_2O_4$ hybrid electrode displays excellent linearity between the steady-state currents and the glucose concentrations in a range of 0.01–21.24 mM with a high sensitivity of 0.3871 $\mu A \cdot \mu M^{-1} \cdot cm^{-2}$. The calibration equation is as follows:

$$j\ (\mathrm{mA \cdot cm^{-2}}) = 0.3871\ C\ (\mathrm{mM}) + 0.0505, (0.01-21.24\ \mathrm{mM}). \quad (9)$$

It is worth noting that the electrode produced a rapid response to the addition of glucose, achieving the steady-state current in less than 1 s, and demonstrates a low LOD of 1 μM at a signal-to-noise ratio of 3 (Fig. 4c). The enhanced performance of the NPG/$NiCo_2O_4$ hybrid electrode can be attributed to its superior conductivity and large active surface area.

Table 1 Comparison of the measured values of serum-glucose concentrations between this work and the hospital

Specimen	Hospital (mM)	This work (mM)	RSD (%)
1	7.93	7.77	3.9
2	17.10	16.93	3.6

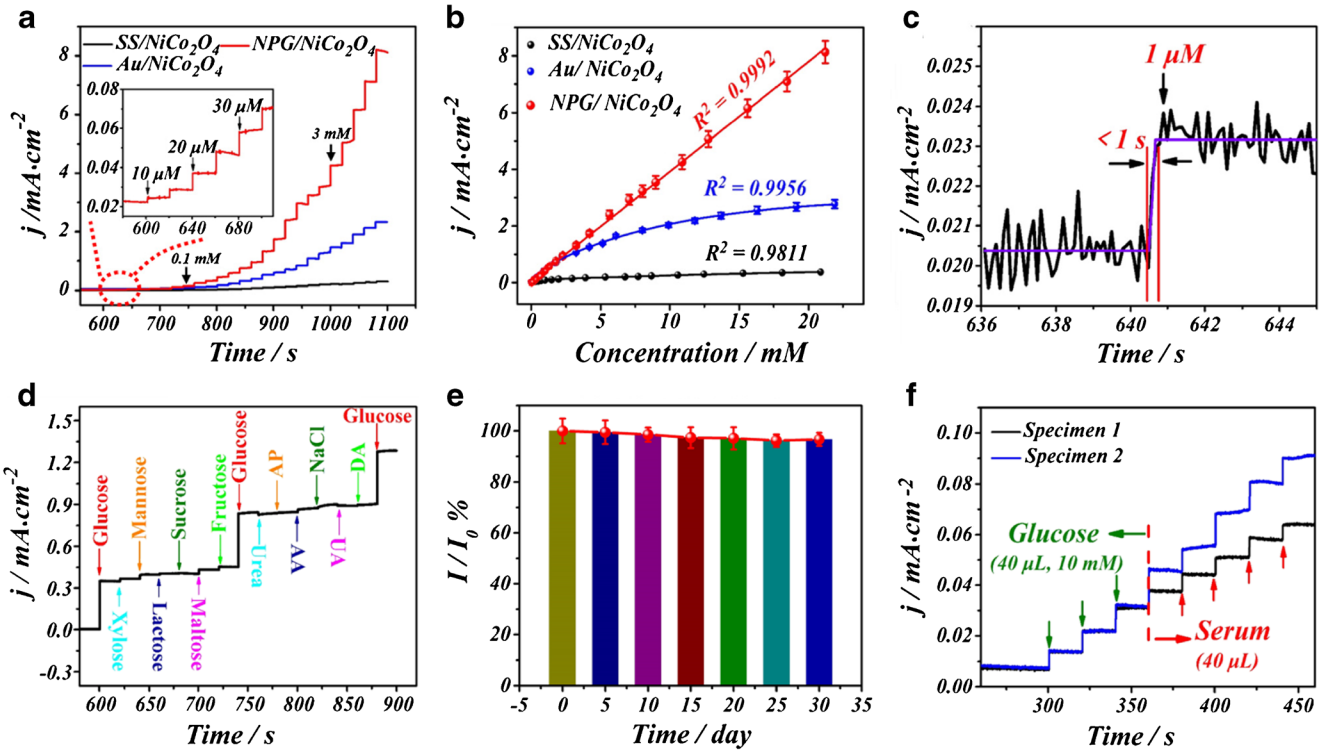

Fig. 4 Amperometric glucose detection. a The amperometric response of the hybrid electrodes to the successive addition of glucose into a 0.1 M NaOH solution at 0.45 V; the inset shows the enlarged response from the red ellipse marked area. **b** The calibration curves for the amperometric responses of the hybrid electrodes. **c** Response time and LOD of the NPG/$NiCo_2O_4$. **d** Amperometric responses to successive additions of 0.1 mM interfering species and 1 mM glucose at a potential of 0.45 V. **e** Long-term stability of the NPG/$NiCo_2O_4$ electrode. **f** The current response of the NPG/$NiCo_2O_4$ needle to three successive additions of 40 μL of glucose (10 mM) and 40 μL of a diabetic patient's blood serum at different times added into 20 mL of a 0.1 M NaOH electrolyte

Table 2 Comparison of the glucose sensing performance of NPG/$NiCo_2O_4$ to the reported literature

Electrode	Sensitivity ($\mu A \cdot \mu M^{-1} \cdot cm^{-2}$)	Linear range (mM)	Potential (V)	Response Time (s)	Reference
$NiCo_2O_4$ nanorods	1.6851	0.0003–1.0	0.6	2	[2]
$NiCo_2O_4$@ Polyaniline	4.5500	0.015–4.735	0.5	5	[18]
$NiCo_2O_4$/3D graphene	2.5240	0.0005–0.59	0.5	_	[29]
Co_3O_4/$NiCo_2O_4$/ graphene	0.304	0.01–3.52	0.55	_	[35]
$Ni(OH)_2$/MoSx	_	0.01–1.3	0.6	2	[36]
Ni-Co NSs/RGO	1.774	0.01–2.65	0.5	_	[37]
Fe_3O_4 nanorod	0.406	0.005–0.766	0.6	_	[38]
	1.341	0.765–3.7			
Ni_3N/Ti	7.688	0.0002–1.5	0.55	5	[39]
NPG/$NiCo_2O_4$	0.3871	0.010–21.24	0.45	<1	This work

Selectivity and stability

The specific detection of glucose is an important parameter for glucose biosensors. As shown in Fig. 4d, the response currents of the prepared electrode were measured by adding 0.1 mM each of urea, AA, DA, UA, AP, NaCl, and other sugars (fructose, lactose, maltose, sucrose, and mannose) into a 1 mM glucose solution, which resulted in only a 0.78–6.7% increase in the current density at 0.45 V. Higher concentrations of 1 mM fructose and 100 mM NaCl were also added into 1 mM glucose solution to test selectivity, indicating the NaCl has little influence on the glucose detection, but fructose produces larger interference, which is the main problem of most of the non-enzymatic glucose biosensors that should be overcome (Fig. S10). Lastly, the current signal increased rapidly after the addition of 1 mM glucose into the interfering species solution, which further confirmed its superior selectivity towards glucose. In addition, the constructed hybrid electrode also displayed good reproducibility and repeatability (Fig. S11). To evaluate the long-term stability of the as-prepared NPG/$NiCo_2O_4$ hybrid electrode, an electrode stored under ambient conditions was measured with 5 mM glucose at five-day intervals. The result shows that there is no obvious decrease of the response signal, retaining approximately 96.66% of its initial current density after one month (Fig. 4e). The morphology is maintained after long-term use of one month based on SEM characterization (Fig. S12). Based on these findings, the excellent repeatability, reproducibility, and stability of the NPG/$NiCo_2O_4$ hybrid electrode make it a promising biosensor for glucose sensing applications.

Analysis of glucose in a serum sample

The selectivity and reliability of the NPG/$NiCo_2O_4$ hybrid electrode were further investigated by analyzing diabetic blood serum with a known glucose concentration. Figure 4f demonstrates the amperometric responses to the successive addition of 40 μL of a 10 mM glucose standard solution and 40 μL of blood serums from diabetic patient into 20 mL of a 0.1 M NaOH solution. Obviously, the amperometric responses of the second specimen are in agreement with that of the first specimen with respect to the addition of the glucose standard solution and the measured concentrations of the serum-glucose mixtures were consistent with that of the hospital clinical results (Table 1). Furthermore, a comparison of the glucose sensing performance between our NPG/$NiCo_2O_4$ hybrid electrode and previous reports for glucose sensing applications is shown in Table 2; all of these results indicate that the NPG/$NiCo_2O_4$ hybrid electrode is an excellent candidate for the detection of glucose in practical biosensor applications.

Conclusions

In summary, a disposable needle-type electrode consisting of stainless steel core and $NiCo_2O_4$ ultrathin nanowalls on nanoporous gold was constructed for electrochemical non-enzymatic glucose biosensing. The consumption cost of gold is reduced and the mechanical strength of the pure NPG wires were highly increased. This hybrid electrode exhibited great performances of rapid response and wide linear range towards glucose oxidation, attributing to the excellent conductivity and a large active surface area from the hierarchical nanoporous structure. The dependence on OH^- for selective glucose oxidation still limits the real implantable application. New catalytic materials should be explored to exhibit sensitive response in neutral solution to overcome this drawback. However, this work provide a novel strategy for fabricating low-cost NPG as a support material for multifunctional applications in the field of catalysis.

Acknowledgements This work was financially supported by the National Key Research and Development Program of China (2016YFA0200400), the Natural Science Foundation of China (51571100, 21275064, 51602305), the Fundamental Research Funds for the Central

Universities, and the Program for JLU Science and Technology Innovative Research Team (JLUSTIRT, 2017TD-09).

Compliance with ethical standards The author(s) declare that they have no competing interests.

References

1. Wang J (2008) Electrochemical glucose biosensors. Chem Rev 108: 814–825
2. Yang J, Cho M, Lee Y (2016) Synthesis of hierarchical $NiCo_2O_4$ hollow nanorods via sacrificial-template accelerate hydrolysis for electrochemical glucose oxidation. Biosens Bioelectron 75:15–22
3. Zheng M, Li L, Gu P, Lin Z, Xue H, Pang H (2017) A glassy carbon electrode modified with ordered nanoporous Co_3O_4 for non-enzymatic sensing of glucose. Microchim Acta 184:943–949
4. Wang Q, Cui X, Chen J, Zheng X, Liu C, Xue T, Wang H, Jin Z, Qiao L, Zheng W (2012) Well-dispersed palladium nanoparticles on graphene oxide as a non-enzymatic glucose sensor. RSC Adv 2: 6245–6249
5. Dhara K, Thiagarajan R, Nair BG, Thekkedath GSB (2015) Highly sensitive and wide-range non-enzymatic disposable glucose sensor based on a screen printed carbon electrode modified with reduced graphene oxide and Pd-CuO nanoparticles. Microchim Acta 182: 2183–2192
6. Julík T, Podešva P, Farka Z, Kováľ D, Skládal P, Foret F (2016) Nanostructured gold deposited in gelatin template applied for electrochemical assay of glucose in serum. Electrochim Acta 188:277–285
7. Zhang H, Liu S (2017) Nanoparticles-assembled NiO nanosheets templated by graphene oxide film for highly sensitive non-enzymatic glucose sensing. Sensors Actuators B Chem 238:788–794
8. Zhao C, Wu X, Li P, Zhao C, Qian X (2017) Hydrothermal deposition of CuO/rGO/Cu_2O nanocomposite on copper foil for sensitive nonenzymatic voltammetric determination of glucose and hydrogen peroxide. Microchim Acta 184:2341–2348
9. Bao L, Li T, Chen S, Peng C, Li L, Xu Q, Chen Y, Ou E, Xu W (2017) 3D graphene frameworks/Co_3O_4 composites electrode for high-performance supercapacitor and enzymeless glucose detection. Small 13:1602077–1602084
10. Gao Z, Zhang L, Ma C, Zhou Q, Tang Y, Tu Z, Yang W, Cui L, Li Y (2016) TiO_2 decorated Co_3O_4 acicular nanotube arrays and its application as a non-enzymatic glucose sensor. Biosens Bioelectron 80:511–518
11. Huo H, Zhao Y, Xu C (2014) 3D Ni_3S_2 nanosheet arrays supported on Ni foam for high-performance supercapacitor and non-enzymatic glucose detection. J Mater Chem A 2:15111–15117
12. Gao Z, Lin Y, He Y, Tang D (2017) Enzyme-free amperometric glucose sensor using a glassy carbon electrode modified with poly(-vinyl butyral) incorporating a hybrid nanostructure composed of molybdenum disulfide and copper sulfide. Microchim Acta 184: 807–814
13. Kim S, Lee SH, Cho M, Lee Y (2016) Solvent-assisted morphology confinement of a nickel sulfide nanostructure and its application for non-enzymatic glucose sensor. Biosens Bioelectron 85:587–595
14. Martín-Yerga D, Carrasco-Rodríguez J, Fierro JLG, García Alonso FJ, Costa-García A (2017) Copper-modified titanium phosphate nanoparticles as electrocatalyst for glucose detection. Electrochim Acta 229:102–111
15. Sun Q, Wang M, Bao S, Wang Y, Gu S (2016) Analysis of cobalt phosphide (CoP) nanorods designed for non-enzyme glucose detection. Analyst 141:256–260
16. Wang Z, Cao X, Liu D, Hao S, Du G, Asiri AM, Sun X (2016) Ternary NiCoP nanosheet array on a Ti mesh: a high-performance electrochemical sensor for glucose detection. Chem Commun 52: 14438–14441
17. Li S, Hou L, Yuan B, Chang M, Ma Y, Du J (2016) Enzyme-free glucose sensor using a glassy carbon electrode modified with reduced graphene oxide decorated with mixed copper and cobalt oxides. Microchim Acta 183:1813–1821
18. Yu Z, Li H, Zhang X, Liu N, Tan W, Zhang X, Zhang L (2016) Facile synthesis of $NiCo_2O_4$@polyaniline core-shell nanocomposite for sensitive determination of glucose. Biosens Bioelectron 75: 161–165
19. Yuan C, Li J, Hou L, Zhang X, Shen L, Lou XWD (2012) Ultrathin mesoporous $NiCo_2O_4$ nanosheets supported on Ni foam as advanced electrodes for supercapacitors. Adv Funct Mater 22:4592–4597
20. Lang X, Fu H, Hou C, Han G, Yang P, Liu Y, Jiang Q (2013) Nanoporous gold supported cobalt oxide microelectrodes as high-performance electrochemical biosensors. Nat Commun 4:2169
21. Ng JWD, García-Melchor M, Bajdich M, Chakthranont P, Kirk C, Vojvodic A, Jaramillo TF (2016) Gold-supported cerium-doped NiOx catalysts for water oxidation. Nat Energy 1:16053
22. Zhou M, Guo S (2015) Electrocatalytic interface based on novel carbon nanomaterials for advanced electrochemical sensors. ChemCatChem 7:2744–2764
23. Duan J, Chen S, Zhao C (2017) Ultrathin metal-organic framework array for efficient electrocatalytic water splitting. Nat Commun 8: 15341
24. Guo M, Yin X, Zhou C, Xia Y, Huang W, Li Z (2014) Ultrasensitive non-enzymatic sensing of glucose on $Ni(OH)_2$-coated nanoporous gold film with two pairs of electron mediators. Electrochim Acta 142:351–358
25. Wu C, Sun H, Li Y, Liu X, Du X, Wang X, Xu P (2015) Biosensor based on glucose oxidase-nanoporous gold co-catalysis for glucose detection. Biosens Bioelectron 66:350–355
26. Jia F, Yu C, Ai Z, Zhang L (2007) Fabrication of nanoporous gold film electrodes with ultrahigh surface area and electrochemical activity. Chem Mater 19:3648–3653
27. Dong X, Xu H, Wang X, Huang Y, Chan-Park MB, Zhang H, Wang L, Huang W, Chen P (2012) 3D graphene-cobalt oxide electrode for high-performance supercapacitor and enzymeless glucose detection. ACS Nano 6:3206–3213
28. Ci S, Huang T, Wen Z, Cui S, Mao S, Steeber DA, Chen J (2014) Nickel oxide hollow microsphere for non-enzyme glucose detection. Biosens Bioelectron 54:251–257
29. Wu M, Meng S, Wang Q, Si W, Huang W, Dong X (2015) Nickel-cobalt oxide decorated three-dimensional graphene as an enzyme mimic for glucose and calcium detection. ACS Appl Mater Interfaces 7:21089–21094
30. Ramachandran K (2016) Ni-Co bimetal nanowires filled multiwalled carbon nanotubes for the highly sensitive and selective non-enzymatic glucose sensor applications. Sci Rep 6:36583
31. Zhan B, Liu C, Chen H, Shi H, Wang L, Chen P, Huang W, Dong X (2014) Free-standing electrochemical electrode based on $Ni(OH)_2$/3D graphene foam for nonenzymatic glucose detection. Nano 6: 7424–7429
32. Qian L, Gu L, Yang L, Yuan H, Xiao D (2013) Direct growth of $NiCo_2O_4$ nanostructures on conductive substrates with enhanced electrocatalytic activity and stability for methanol oxidation. Nano 5:7388–7396
33. Xu X, Song F, Hu X (2016) A nickel iron diselenide-derived efficient oxygen-evolution catalyst. Nat Commun 7:12324
34. Lei F, Liu W, Sun Y, Xu J, Liu K, Liang L, Yao T, Pan B, Wei S, Xie Y (2016) Metallic tin quantum sheets confined in graphene toward high-efficiency carbon dioxide electroreduction. Nat Commun 7: 12697

35. Xue B, Li K, Feng L, Lu J, Zhang L (2017) Graphene wrapped porous $Co_3O_4/NiCo_2O_4$ double-shelled nanocages with enhanced electrocatalytic performance for glucose sensor. Electrochim Acta 239:36–44
36. Ji S, Yang Z, Zhang C, Miao Y, Tjiu WW, Pan J, Liu T (2013) Nonenzymatic sensor for glucose based on a glassy carbon electrode modified with $Ni(OH)_2$ nanoparticles grown on a film of molybdenum sulfide. Microchim Acta 180:1127–1134
37. Wang L, Lu X, Ye Y, Sun L, Song Y (2013) Nickel-cobalt nanostructures coated reduced graphene oxide nanocomposite electrode for nonenzymatic glucose biosensing. Electrochim Acta 114:484–493
38. Zhang C, Ni H, Chen R, Zhan W, Zhang B, Lei R, Xiao T, Zha Y (2015) Enzyme-free glucose sensing based on Fe_3O_4 nanorod arrays. Microchim Acta 182:1811–1818
39. Xie F, Liu T, Xie L, Sun X, Luo Y (2018) Metallic nickel nitride nanosheet: an efficient catalyst electrode for sensitive and selective non-enzymatic glucose sensing. Sensors Actuators B Chem 255: 2794–2799